Journal of Analytical and Applied Pyrolysis 96 (2012) 126–138

Contents lists available at SciVerse ScienceDirect

Journal of Analytical and Applied Pyrolysis

journal homepage: www.elsevier.com/locate/jaap

Predicting the pyrolysis of single biomass particles based on a time and space integral method

Y. Haseli*, J.A. van Oijen, L.P.H. de Goey

Combustion Technology, Department of Mechanical Engineering, Eindhoven University of Technology, PO Box 513, 5600 MB Eindhoven, The Netherlands

ARTICLE INFO

Article history:
Received 7 December 2011
Accepted 25 March 2012
Available online 3 April 2012

Keywords:
Pyrolysis
Simplified model
Thermally thin particle
Pyrolysis temperature
Time and space integral method

ABSTRACT

The objective of this paper is to present a simple pyrolysis model to capture the main characteristics of the decomposition of a thermally thin particle at high temperatures corresponding to those found in the furnace of coal/biomass power plants. To achieve this goal, it is assumed that pyrolysis begins soon after the surface of the particle has reached a certain pyrolysis temperature, and proceeds according to a shrinking (unreacted) core model with an infinitesimal reaction front. The formulation of various stages including initial heating, pre-pyrolysis heating, pyrolysis and post-pyrolysis heating is carried out based on a time and space integral method which allows one to describe the energy conservation equation in an algebraic form. Two different treatments are presented for the pyrolysis stage. The first formulation assumes separate temperature profiles for char and biomass regions (double-temperature profile), whereas in the second treatment only one profile is considered for the temperature throughout the particle (single-temperature profile). Of particular interest is the latter approach that leads to simple relationships for predicting the duration of various stages, enabling one to predict the mass loss history. The accuracy of both methods is examined by comparing their predictions with recent experimental data reported in the literature as well as the prediction of comprehensive pyrolysis models. Satisfactory agreement is achieved indicating that both pyrolysis models based on double- and single-temperature profiles can be used with sufficient accuracy for engineering purposes.

© 2012 Elsevier B.V. All rights reserved.

1. Introduction

Thermochemical conversion of biomass is a topic of technological importance due to the increasing interest in the utilization of biomass as a renewable energy source. The main mechanism for chemically converting the biomass into other byproducts is heat from an external source. The energy from biomass can either be directly converted into heat, for instance, in the furnace of a power plant, or into the liquid fuel and biogas within a gasifier. The well-established methods of thermochemical conversion of biomass for engineering applications include combustion, gasification, torrefaction and pyrolysis. The key differences between these methods are related to the oxygen concentration in the surrounding fluid and the operating temperature.

A substantial amount of research has been conducted on the subject of biomass pyrolysis by means of experimental and numerical investigations to increase the knowledge of various physical and chemical processes involved in the biomass pyrolysis. The reader may access the recent state-of-the art in Refs. [1–12]. The common feature of the models reported in these references is that the transport equations are usually described one-dimensionally and combined with a kinetic scheme representing chemistry of the virgin biomass decomposition. Two and three-dimensional models have rarely been reported; see e.g. Ghabi et al. [13]. The advantage of these models is that they allow calculating a variety of parameters such as solid and gas phase densities, temperature, pressure and velocity fields within the porous matrix and formation of main byproducts (light gases, tar and char) in space and time. Such advanced models enable one to get a deeper understanding of the physics and chemistry of the pyrolysis process on the scale of a single particle.

Because of the transient nature of the pyrolysis process, the transport equations are necessarily described in partial differential forms in order to capture the variation of key parameters along the particle and during the process. This would be at the expense of considerable amount of computational and programming efforts, in particular, when dealing with design of combustors and gasifiers, where a large number of particles undergo thermochemical conversion. For practical applications, designers are commonly interested in only a few parameters such as average temperature and/or temperature at the surface of the particle, rate and the amount of particle mass loss, ignition time at which a particle begins to

---

* Corresponding author.
E-mail address: y.haseli@tue.nl (Y. Haseli).

0165-2370/$ – see front matter © 2012 Elsevier B.V. All rights reserved.
http://dx.doi.org/10.1016/j.jaap.2012.03.014

Nomenclature

c_p	specific heat (J/kg K)
h	convective heat transfer coefficient (W/m^2 K)
k	thermal conductivity (W/m K)
L	thickness/Length of particle (m)
L_{cr}	minimum particle length for transition from thermally thin to thermally thick regime (m)
$\dot{m}''$	decomposition rate per unit surface area (kg/m^2 s)
q''	heat flux (W/m^2)
q''_{net}	net heat flux at particle surface (W/m^2)
R	particle radius (m)
T	temperature (K)
T_p	pyrolysis temperature (K)
T_s	surface temperature (K)
T_{sL}	surface temperature at the time t_L (K)
t	time (s)
t_L	duration of thermal penetration movement from the front surface to the back face of the particle (s)
$t_{p,ini}$	time of commencement of pyrolysis at the surface of particle (s)
t_p	conversion/pyrolysis time (s)
x	spatial coordinate
x_c	char depth (m)
x_t	thermal penetration depth (m)

Greek letters

α	thermal diffusivity (m^2/s)
Δh_p	specific enthalpy of pyrolysis (J/kg)
ε	emissivity
ρ	density (kg/m^3)
σ	Stephen–Boltzmann coefficient (W/m^2 K^4)
φ	coefficient of Eqs. (3) and (17)
ψ	coefficients of Eq. (16)

Subscripts

0	initial condition
∞	surrounding condition
B	biomass
BC	boundary condition
C	char
ext	external
f	final
ph	post-pyrolysis heating up
r	reactor

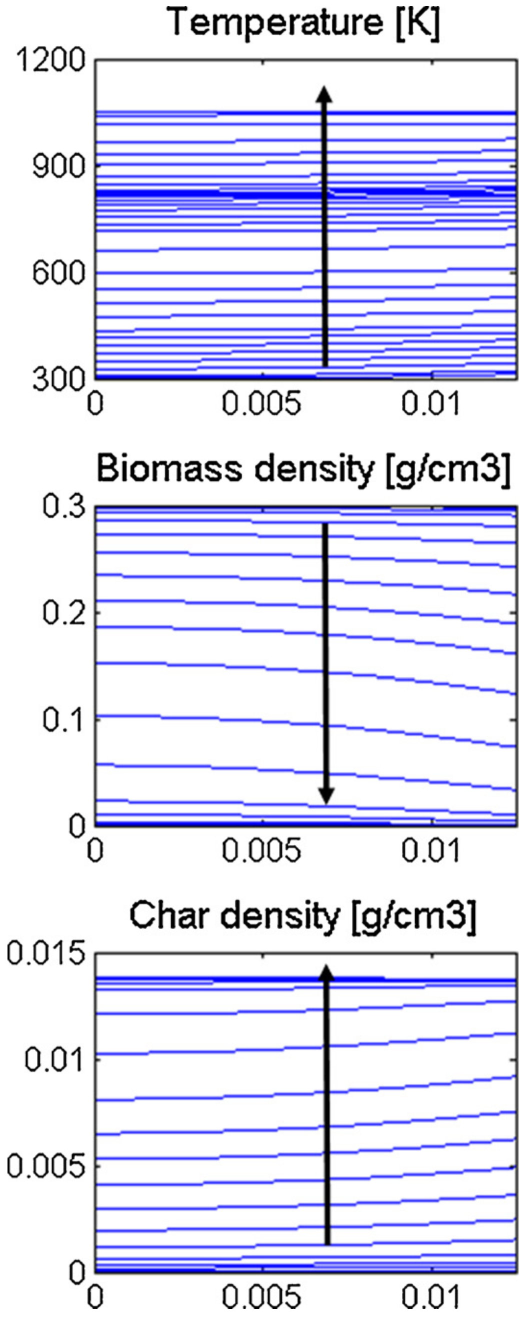

Fig. 1. Illustrative time and space evolution of intra-particle gradients of a biomass particle undergoing a homogenous pyrolysis (250 μm; 1050 K; 300 kg/m^3). Different lines correspond to different times increasing in the direction of the arrows.

decompose, and total duration of the conversion process. To capture the main characteristics of the pyrolysis of solid fuels with optimized computational efforts requires one to employ less complex models.

From a mathematical point of view, a key step towards simplified pyrolysis models is to describe the particle conversion process in the form of a set of ordinary differential equations (ODEs) rather than partial differential equations (PDEs). In principle, a chemically converting solid particle may ultimately decompose in the following two extreme limits: the regime of shrinking density, and the shrinking core regime. In the former limit, a particle undergoes an almost homogenous conversion in the absence of intra-particle gradients, whereas in the latter extreme limit the reaction takes place at a very thin layer, resulting in a reaction front that is created at the surface of the particle and moves towards its center.

For the case of pyrolysis of charring materials, e.g. wood, a particle may decompose homogeneously in the regime of kinetically controlled conversion. Our previous study [2] indicated that homogenous pyrolysis of a wood particle may occur at low densities, small particles and low operational temperatures corresponding to (typically for a cylindrical beech wood) $\mathrm{Bi} < 0.1$ and $\mathrm{Py}' > 1.5 \times 10^{-3}$, where Bi and Py' denote Biot and the external pyrolysis numbers, respectively. A typical time and space evolution of biomass and char densities as well as temperature of a particle undergoing a homogenous pyrolysis predicted by a comprehensive pyrolysis model [1,2] is depicted in Fig. 1.

It is however unlikely that pyrolysis of biomass in combustors and gasifiers occurs in the regime of kinetically controlled in the absence of intra-particle gradients, due to the high operational temperatures and relatively large particles. It is difficult to mill biomass due to its fibrous structure which results in particles of relatively large size (around 1 mm). Moreover, Lu et al. [14] and Bharadwaj et al. [15] examined the accuracy of a lumped model (treating the particle as a whole) and found significant errors in the predictions indicating that the intra-particle effects need to be accounted for in a pyrolysis model.

Based on the arguments provided in Refs. [2,14,15], one needs to account for the temperature gradients inside a pyrolyzing particle. A recent study by Saastamoinen et al. [16] has also revealed that the intra-particle gradients of particles of less than a millimeter in real furnaces can be significant. The pyrolysis model employed by Saastamoinen et al. [16] assumes that the density of particle decreases homogeneously throughout the particle. To account for internal temperature gradients their model incorporates an internal thermal resistance in terms of particle thermal conductivity and size.

Another case is to employ the concept of shrinking core model assuming that the pyrolysis begins as soon as the surface temperature reaches a characteristics temperature T_p (to be called pyrolysis temperature throughout this article), thereby yielding a reaction front. A further simplifying assumption is that the virgin biomass decomposes to char and volatiles at an infinite rate in a very thin layer dividing the particle into char layer and biomass region. To account for the temperature gradient inside the particle, one may employ the concept of integral method that was originally proposed by Goodman [17]. This method allows one to describe a one-dimensional transient heat transfer problem represented in terms of a partial differential equation (PDE), in the form of an ordinary differential equation (ODE).

The integral method is based on an assumption for the spatial behavior of the temperature along the particle, so that upon integrating the energy equation over the space coordinate the particle pyrolysis model is converted into an ODE. This method has been used for predicting the pyrolysis of solid particles in some past studies [18–26]. Although the concept of the shrinking core model has been commonly employed in these studies, the essential differences between them are summarized in Table 1. Furthermore, the formulation and solution methodology differ from one study to another. For instance, an infinite decomposition rate at a constant pyrolysis temperature assumption is adopted in Refs. [18–24]. On the other hand, Galgano and Di Blasi [25,26] used a finite rate model of conversion for cylindrical wood particles.

Given that the concept of a fixed pyrolysis temperature T_p may seem to be controversial, it is a useful simplifying approach, in particular, when dealing with flaming combustion [27]. Furthermore, Galgano and Di Blasi [28] assessed the predictions of a shrinking core model with both finite rate and infinite rate pyrolysis models. They found that the unknown temperature T_p is not necessarily the same as that predicted by the finite rate model. However, the main conclusion was that the most important process characteristics could be accurately predicted by assigning a proper value for T_p.

A careful review of the above cited sources indicates that the concept of shrinking core model has been only used for predicting the pyrolysis of *thermally thick* particles in which ignition takes place at the particle surface before thermal penetration reaches the back face. A further possible situation which has not been fully realized in past studies is the case in which the ignition occurs after thermal penetration has reached the back face. In this study, this will be referred to as *thermally thin* particle. More importantly, the various stages of conversion of a finite size particle have not been adequately described. These observations form the primary motivation of the present study to develop simple models for a finite size thermally thin wood particle undergoing a pyrolysis process. The main objective is to introduce a novel modeling approach based on a *time and space integral method*, which can be easily linked with CFD models for designing combustors and gasifiers of solid particles. It will be shown that the model presented in this paper is much simpler and easier for coding compared to those presented by others.

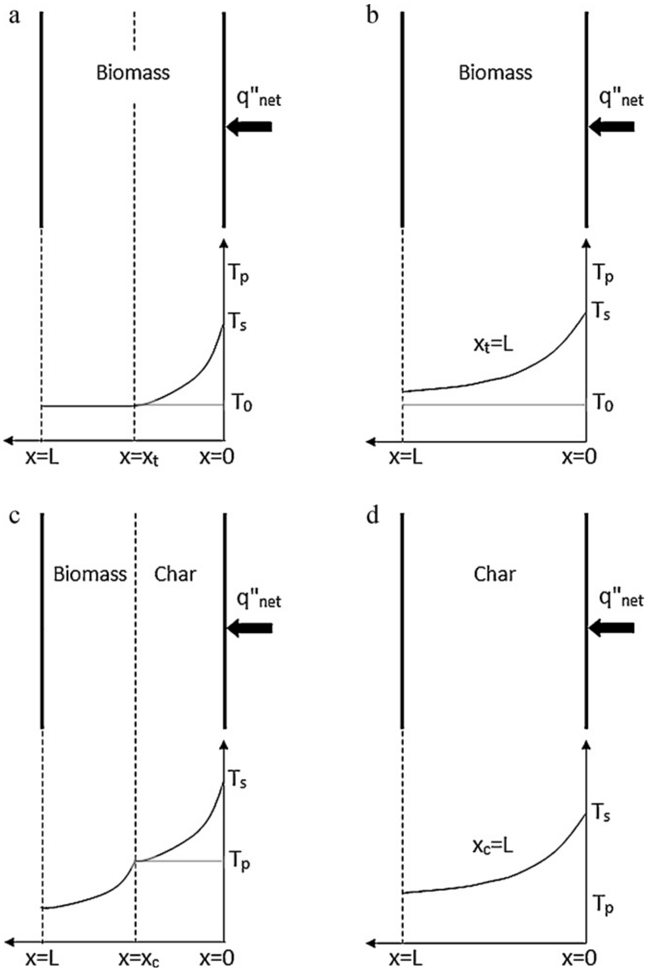

Fig. 2. Schematic representation of a pyrolyzing thermally thin particle.

In the upcoming section, we first explain the sub-processes involved in the pyrolysis of a thermally thin particle. The formulation of various stages will be subsequently presented in Section 3. Typical numerical results and the validation of the new model against different experiments and the prediction of a comprehensive model will be given in Section 4. Finally, Section 5 deals with the evaluation of the model results and its accuracy.

2. Description of the process

Consider a dry slab biomass particle with a thickness of L that is exposed to a hot environment. The particle is initially at temperature T_0 ($<T_p$), and it is assumed that the pyrolysis begins as soon as the surface temperature reaches the pyrolysis temperature T_p. Further assumptions taken into account in the development of the present model (Section 3) are: (1) particle volume remains unchanged during the entire process; (2) thermo-physical properties are constant; (3) pyrolysis takes place at a very thin layer where the temperature is T_p; (4) the convective flow of volatiles is neglected.

Depending on particle size, thermo-physical properties and external heating rate, the particle may experience two different conversion regimes as depicted in Figs. 2 and 3. Initially, the particle begins to heat up so that a thermal wave with a thickness x_t measured from the surface is formed. One possible situation is that the thermal wave reaches the back face (assumed to be insulated in

Table 1
The specification of the integral method employed in past studies.

Researcher(s)	Temperature profile	Particle	Validation against
Kanury [18]	Linear	Charring slab and cylinder	Experiments
Chen et al. [19]	Exponential	Charring and non-charring finite slab	Analytical solution
Quintiere and Iqbal [20]	Quadratic	Non-charring semi-infinite slab	Experiments and PDE model
Weng et al. [21]	Linear (char layer) and quadratic (virgin layer)	Charring semi-infinite slab	Experiments of wood pyrolysis with char oxidation
Spearpoint and Quintiere [22]	Linear (char layer) and quadratic (virgin layer)	Charring semi-infinite slab	Experiments of different pyrolyzing woods
Galgano and Di Blasi [24]	Quadratic	Charring cylinder	Experiments of wood pyrolysis

this study); i.e. x_t equals L, while the surface temperature T_s is still less than T_p (see Fig. 2b). The heating up process continues until T_s becomes T_p; at this moment the surface of the particle decomposes to volatiles and char residue. On the other hand, a second possibility is that the thermal wave is still moving towards the back face of the particle while T_s has already reached T_p (see Fig. 3b). In order to avoid any confusion, we intentionally distinguish between these two situations; the first case will be referred to as *thermally thin particle*, and the second one as *thermally thick particle*.

A thermally thin particle undergoes the following four stages:

1. Initial heating up (Fig. 2a),
2. Pre-pyrolysis heating up (Fig. 2b),
3. Pyrolysis (Fig. 2c),
4. Post-pyrolysis heating up (Fig. 2d).

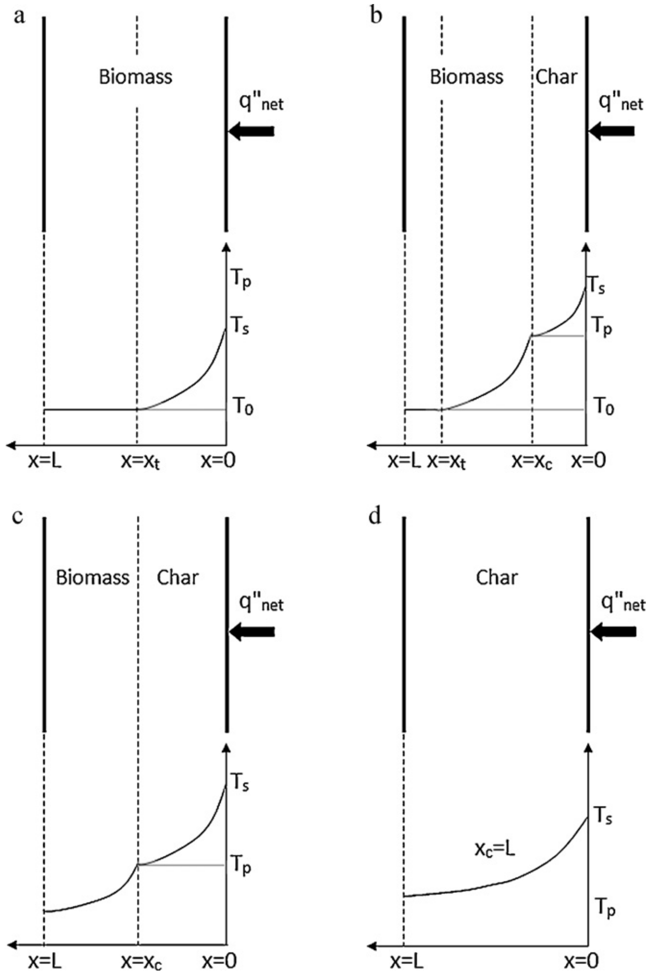

Fig. 3. Schematic representation of a pyrolyzing thermally thick particle.

In the first stage of the process, a thermal wave (Fig. 2a) is created at the surface and it moves inside of the particle as the time passes until it reaches the back face; i.e. $x_t = L$, at the time t_L while the surface temperature is still less than T_p. As shown in Fig. 2b, the heating up process continues until T_s reaches T_p; whereby initiating the pyrolysis process at the surface of the particle. The time required for the surface of the particle to reach the pyrolysis temperature is denoted by $t_{p,ini}$. From this moment on, the particle is divided into two regions: the virgin part, which still undergoes the heating up process, and the char layer with thickness x_c (Fig. 2c). The pyrolysis front propagates inside the particle by continuation of the process so that the thickness of the char region increases until time t_p at which x_c equals L. At this moment the virgin biomass has completely converted to char and volatiles assumed to leave the particle immediately upon formation. The final stage is the char heating up (post-pyrolysis stage) as depicted in Fig. 2d. So, the problem is a simple conduction heat transfer. This stage will cease when thermal equilibrium between the particle and surrounding is established.

As pointed out earlier, for a thermally thick particle the process is a little different (see Fig. 3) in a way that after initiation of the heating up stage (Fig. 3a), the surface temperature increases up to T_p before the thermal wave reaches the back face. In other words, for a thermally thick particle $t_L > t_{p,ini}$. Thus, upon initiation of the pyrolysis process, the particle is divided into three regions: char layer ($0 < x < x_c$), virgin biomass undergoing heating up process ($x_c < x < x_t$), and virgin biomass maintained at the initial temperature ($x_t < x < L$). By continuation of the pyrolysis process, the thermal wave and the char front penetrate into the particle until x_t reaches the back face. Beyond this moment, the rest of the process is the same as the thermally thin particle as depicted in Fig. 3c and d. In summary, the following processes take place in a thermally thick particle:

1. Initial heating up (Fig. 3a),
2. Heating-pyrolysis (Fig. 3b),
3. Pyrolysis (Fig. 3c),
4. Post-pyrolysis heating up (Fig. 3d).

The focus of the present study is on thermally thin particles. In the upcoming section, the formulation of the four stages of the pyrolysis process will be presented using a time and space integral method.

3. Formulation

The main basis for model development is that the temperature within the particle will be assumed to obey a quadratic function satisfying the boundary conditions. The assumption of decomposition of virgin biomass in an infinitesimal thin layer whose temperature is represented by T_p leads to simply describe the heat transfer equation in terms of transient conduction problem in both char and biomass layers. Upon integrating the heat transfer equation with respect to the space coordinate, the PDE form of energy equation reduces to an ODE with respect to time. In the next step, time integration is applied to the resulted ODE which leads to an algebraic equation. This approach will be used in all stages of the conversion process depicted in Fig. 2.

3.1. Initial heating up

As the particle undergoes a transient conduction process (Fig. 2a), the conservation of energy can be represented as follows:

$$\frac{\partial T}{\partial t} = \alpha_B \frac{\partial^2 T}{\partial x^2}, \tag{1}$$

where $\alpha_B = k_B/(\rho_B c_{pB})$.

The following initial and boundary conditions are prescribed for this problem:

$$\text{Initial condition}: \quad T = T_0 \quad \text{at} \quad t = 0.$$

$$\begin{aligned} \text{Boundary condition}: \quad & \text{BC}_1: \quad -k_B \frac{\partial T}{\partial x}|_{x=0} = q''_{net}, \\ & \text{BC}_2: \quad k_B \frac{\partial T}{\partial x}|_{x=x_t} = 0, \\ & \text{BC}_3: \quad T|_{x=x_t} = T_0. \end{aligned}$$

For a known external radiant heat flux q''_{ext}, the net heat flux at the surface of the particle is:

$$q''_{net} = q''_{ext} - h(T_s - T_\infty) - \sigma\varepsilon(T_s^4 - T_\infty^4). \tag{2a}$$

On the other hand, for a known reactor temperature T_r, the net heat flux is described as:

$$q''_{net} = h(T_r - T_s) + \sigma\varepsilon(T_r^4 - T_s^4). \tag{2b}$$

As mentioned earlier, the temperature profile is assumed to obey a quadratic function at each instant. Hence,

$$T = \phi_2 x^2 + \phi_1 x + \phi_0, \tag{3}$$

where the coefficients of Eq. (3) are functions of time. With the aid of the boundary conditions mentioned above, these coefficients can be obtained so that the resulting temperature profile obeys:

$$T = T_0 + \frac{q''_{net}}{2k_B} x_t \left(1 - \frac{x}{x_t}\right)^2. \tag{4}$$

Applying a space integration to Eq. (1) from $x = 0$ to $x = x_t$ yields:

$$\frac{d}{dt}\left(\int_0^{x_t} T dx - T_0 \frac{dx_t}{dt}\right) = \alpha_B \left(\frac{\partial T}{\partial x}|_{x=x_t} - \frac{\partial T}{\partial x}|_{x=0}\right). \tag{5}$$

Using Eq. (4) and the boundary conditions, Eq. (5) reduces to:

$$\frac{d}{dt}(q''_{net} x_t^2) = 6\alpha_B q''_{net} \tag{6}$$

Applying approximate time integration to Eq. (6) using a mean value for q''_{net} $(= [q''_{net} + q''_0]/2)$ leads to:

$$x_t(t) = \sqrt{3\alpha_B \left[1 + \frac{q''_0}{q''_{net}}\right] t}. \tag{7}$$

where q''_0 denotes the net heat flux at $t = 0$. Note that the net heat flux is a function of T_s which is obtained from the temperature profile relationship; i.e. Eq. (4). Hence,

$$T_s(t) = T_0 + \frac{q''_{net}}{2k_B} x_t. \tag{8}$$

The time required for the thermal wave to reach the back face is obtained by inserting $x_t = L$ into Eq. (7). Hence,

$$t_L = \frac{L^2}{3\alpha_B[1 + (q''_0/q''_{net})]}. \tag{9}$$

For a thermally thin particle, t_L is less than $t_{p,ini}$. At a given process condition, it is possible to determine the particle thickness at which t_L equals $t_{p,ini}$. To determine the time at which T_s reaches T_p; i.e. initiation of pyrolysis, one should first eliminate x_t between Eqs. (7) and (8), rearrange the resulting expression for t and replace T_s by T_p. Hence,

$$t_{p,ini} = \frac{(T_p - T_0)^2}{3\alpha_B (q''_{net}/2k_B)^2 (1 + (q''_0/q''_{net}))}. \tag{10}$$

Equating the right hand sides of Eqs. (9) and (10) and rearranging for L gives:

$$L_{cr} = 2k_B \left(\frac{T_p - T_0}{q''_{net}}\right). \tag{11}$$

L_{cr} denotes the minimum size of the particle for transition from thermally thin to thermally thick regime. Notice that for a particle heated uniformly in a reactor from both sides, L (and L_{cr}) would exhibit half of the particle thickness.

In fact, Eq. (11) allows one to identify whether a particle is thermally thin or thermally thick. If the particle size is less than L_{cr}, the problem under study is characterized with the regime of thermally thin otherwise the particle is thermally thick. It should be noted that for a thermally thin particle ($L < L_{cr}$), $t_{p,ini}$ has to be obtained from the next stage of the formulation to be followed in the subsequent section.

Typically, thermal conductivity of various biomass types is between 0.2 and 0.4 W/m K, the pyrolysis temperature varies in the range of 523–773 K, and the reactor temperature is above 1200 K. For instance, assume $T_p = 673$ K, $T_0 = 300$ K, $k_B = 0.25$ W/m K, $T_r = 1273$ K, $h = 15$ W/m^2 K. Using Eq. (2b), the net heat flux at the surface of the particle at the time of initiation of pyrolysis is 146 kW. Inserting the above values in Eq. (11) gives $L_{cr} = 1.3$ mm, which is equivalent to a particle thickness of 2.6 mm if the particle is heated from both sides. In practice, such as in power plant furnaces, the particle thickness is usually less than 1 mm for raw biomass particles. In the case of torrefied biomass, the particle size is expected to be even smaller; e.g. less than 0.5 mm. This sample calculation indicates that the regime of particle pyrolysis in real combustors is thermally thin (Fig. 2) since the particle thickness is less than its critical value. It is obvious that depending on ignition temperature, thermal conductivity and heating condition, the value of L_{cr} would be different. Typical values of the critical half thickness of a particle are depicted in Fig. 4, which supports the idea that the pyrolysis of (raw and torrefied) biomass particles in most real furnaces occurs in a thermally thin regime.

3.2. Pre-pyrolysis heating up

In the second phase of heating up process, the thermal wave has already reached the back face while T_s is still less than T_p (see Fig. 2b). A similar procedure as explained above is undertaken. That is, the problem is still described by Eq. (1) assuming that the temperature profile can be approximated with Eq. (3). The following initial and boundary conditions are applied:

$$\text{Initial condition}: \quad T_s = T_{s,L} \quad \text{at} \quad t = t_L.$$

$$\begin{aligned} \text{Boundary condition}: \quad & \text{BC}_1: \quad -k_B \frac{\partial T}{\partial x}|_{x=0} = q''_{net}, \\ & \text{BC}_2: \quad k_B \frac{\partial T}{\partial x}|_{x=L} = 0, \\ & \text{BC}_3: \quad T|_{x=0} = T_s. \end{aligned}$$

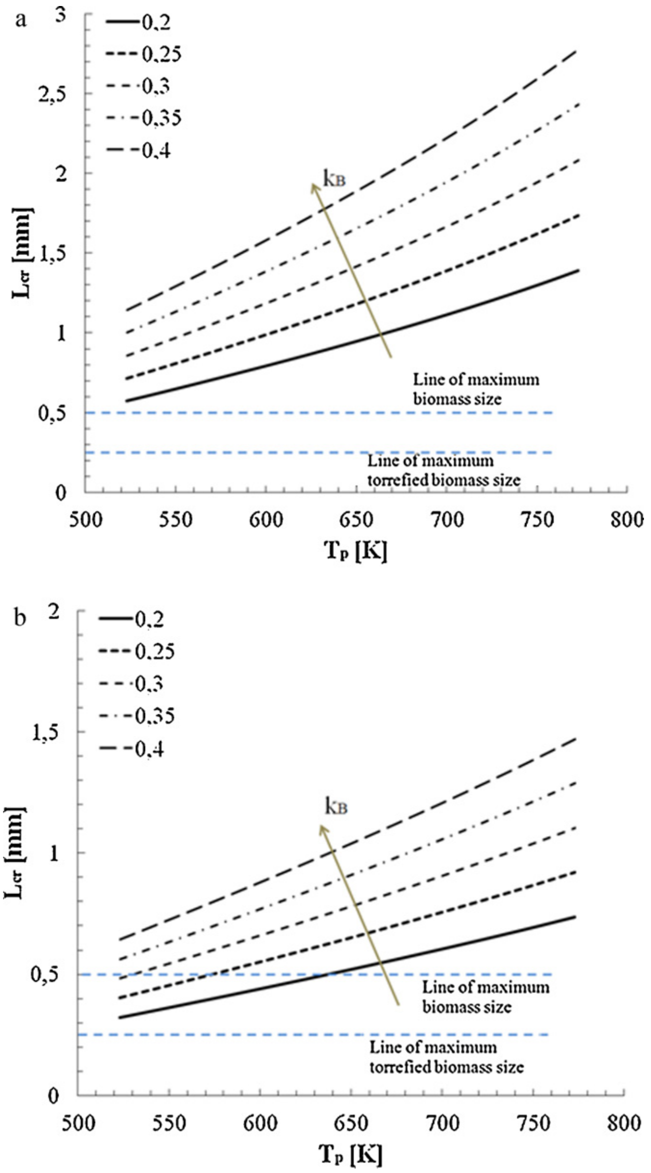

Fig. 4. Critical half thickness of particle versus ignition temperature at varying thermal conductivity at a reactor temperature of (a) 1273 K, and (b) 1473 K.

Upon determining the coefficients of Eq. (3) with the aid of the above boundary conditions, the temperature takes the following form as a function of x:

$$T = T_s - \frac{q''_{net}}{k_B}x + \frac{q''_{net}}{2k_B L}x^2. \tag{12}$$

Integrating Eq. (1) with respect to x along the particle thickness, and inserting Eq. (12) into the resulting expression yields:

$$\frac{d}{dt}\left[T_s L - \frac{q''_{net}}{3k_B}L^2\right] = \alpha_B \frac{q''_{net}}{k_B}. \tag{13}$$

Integrating Eq. (13) with respect to the time from t_L to t, and assuming a mean value for q''_{net} equaling $(q''_{net} + q''_L)/2$) leads to the following relationship:

$$T_s = T_{s,L} + (q''_{net} - q''_L)\frac{L}{3k_B} + \frac{\alpha_B}{2k_B L}(q''_{net} + q''_L)(t - t_L), \tag{14}$$

where the surface temperature and the net heat flux at the time t_L; i.e. $T_{s,L}$ and q''_L, are obtained from the previous heating up phase.

To determine the time at which the pyrolysis initiates at the surface, one needs to solve Eq. (14) for t with $T_s = T_p$. This leads to:

$$t_{p,ini} = t_L + \left[T_p - T_{sL} - (q''_{p,ini} - q''_L)\frac{L}{3k_B}\right]\frac{2k_B L}{\alpha_B(q''_{p,ini} + q''_L)}, \tag{15}$$

where $q''_{p,ini}$ is the net surface heat flux at the time of initiation of pyrolysis to be calculated using Eq (2) with $T_s = T_p$, T_{sL} denotes the surface temperature at t_L which can be determined from Eqs. (2) and (8) with $x_t = L$, and q''_L is the net surface heat flux at the time t_L to be obtained from Eq (2) with $T_s = T_{sL}$.

3.3. *Pyrolysis*

The formulation presented in the previous section is valid until initiation of pyrolysis at the surface of the particle. According to Fig. 2c, the particle consists of a char region with thickness x_c and a virgin biomass region with length $L - x_c$. The temperature at the virgin/char interface, where the pyrolysis takes place at infinitesimal rate, is T_p. Consistent with the analysis presented for the heating up stage, the temperature inside the particle is assumed to obey a quadratic function. Two treatments will be presented: Double-temperature profile, and single-temperature profile. In the former case, separate temperature profiles are considered for biomass and char regions, whereas in the case of single temperature profile, only one spatial profile is assumed for temperature throughout the particle.

3.3.1. *Double-temperature profile*

Let us first consider the case of double-temperature profile such that the temperature profiles in the char and biomass layers are represented as follows:

$$\text{Char region}(0 \le x \le x_c): \quad T_C = \psi_2(x_c - x)^2 + \psi_1(x_c - x) + \psi_0. \tag{16}$$

$$\text{Biomass region}(x_c \le x \le L): \quad T_B = \phi_2(x - x_c)^2 + \phi_1(x - x_c) + \phi_0. \tag{17}$$

The heat transfer equation in the biomass region is still represented by Eq. (1). A similar equation can be prescribed for the char layer.

$$\frac{\partial T}{\partial t} = \alpha_C \frac{\partial^2 T}{\partial x^2}, \tag{18}$$

where $\alpha_C = k_C/(\rho_C c_{pC})$.

By applying the following boundary conditions,

$$\mathrm{BC}_1: -k_C \frac{\partial T_C}{\partial x}|_{x=0} = q''_{net},$$

$$\mathrm{BC}_2: \frac{\partial T_B}{\partial x}|_{x=L} = 0,$$

$$\mathrm{BC}_3: T_B|_{x=x_c} = T_C|_{x=x_c} = T_p,$$

$$\mathrm{BC}_4: -k_B \frac{\partial T_B}{\partial x}|_{x=x_c} = -k_C \frac{\partial T_C}{\partial x}|_{x=x_c} + \dot{m}''\Delta h_p,$$

and determining the coefficients ψ_i and ϕ_i, Eqs. (16) and (17) are rewritten as:

$$T_C = T_p - \frac{k_B\phi_1 + \dot{m}''\Delta h_p}{k_C}(x_c - x) + \frac{q''_{net} + k_B\phi_1 + \dot{m}''\Delta h_p}{2x_c k_C}(x_c - x)^2, \tag{19}$$

$$T_B = T_p + \phi_1(x - x_c) - \frac{\phi_1}{2(L - x_c)}(x - x_c)^2, \tag{20}$$

where Δh_p denotes the specific heat of pyrolysis (negative when endothermic and positive when exothermic), and $\dot{m}''$ represents the decomposition rate per unit particle surface area perpendicular to x-coordinate.

$$\dot{m}'' = \rho_B \frac{\Delta x_c}{\Delta t}, \tag{21}$$

where Δt is a very small increment of time.

Initially; i.e. $t = t_{p,ini}$, $x_c = 0$ and $\phi_1 = -q''_p/k_B$. Integrating Eq. (18) with respect to x between $x = 0$ and $x = x_c$, and using boundary conditions and temperature profiles given in Eq. (19) yields:

$$\frac{d}{dt}[(q''_{net} - 2k_B\phi_1 - 2\dot{m}''\Delta h_p)x_c^2] = 6\alpha_C(q''_{net} + k_B\phi_1 + \dot{m}''\Delta h_p). \tag{22}$$

Approximate time integration of Eq. (22) from $t_{p,ini}$ to t gives:

$$x_c = \sqrt{3\alpha_C\left(\frac{q''_{net} + k_B\phi_1 + \dot{m}''\Delta h_p}{q''_{net} - 2k_B\phi_1 - 2\dot{m}''\Delta h_p}\right)(t - t_{p,ini})}. \tag{23}$$

Note that a mean value for the terms inside the bracket on the right hand side of Eq. (22) is considered when performing the time integration.

Likewise, integrating Eq. (1) between $x = x_c$ and $x = L$ using Eq. (20) results in:

$$\frac{d}{dt}[\phi_1(L - x_c)^2] = -3\alpha_B\phi_1. \tag{24}$$

After applying approximate time integration from $t - \Delta t$ to t and some rearrangements, a solution of Eq. (24) over a small time increment Δt is found:

$$\phi_1(t) = \phi_1(t - \Delta t)\left[\frac{L - x_c(t - \Delta t)}{L - x_c(t)}\right]^2 \exp\left[-\frac{3\alpha_B \Delta t}{(L - \bar{x}_c)^2}\right], \tag{25}$$

where $\bar{x}_c = [x_c(t) + x_c(t - \Delta t)]/2$.

At each instant, the surface temperature is determined from Eq. (19) with $x = 0$. Hence,

$$T_s = T_p + \left(\frac{q''_{net} - k_B\phi_1 - \dot{m}''\Delta h_p}{2k_C}\right)x_c. \tag{26}$$

3.3.2. *Single-temperature profile*

Similar to the analysis presented in Sections 3.1 and 3.2, we assume that the temperature profile throughout the particle is represented by Eq. (3) whose coefficients can be obtained with the appropriate boundary conditions at the particle surface and back face, and at the location of x_c where the temperature is T_p, thereby resulting in:

$$T = T_p - \frac{q''_{net}}{k_C}\frac{L - x_c}{L}(x - x_c) + \frac{q''_{net}}{2k_C L}(x - x_c)^2. \tag{27}$$

From conservation of energy for the particle, the net change in the energy of the particle is equal to the net amount of energy transferred to the particle. This would lead to:

$$\rho_B c_{pB}\frac{d}{dt}\int_{x_c}^{L} T dx + \rho_B c_{pB} T_p \frac{dx_c}{dt} + \rho_C c_{pC}\frac{d}{dt}\int_0^{x_c} T dx - \rho_C c_{pC} T_p \frac{dx_c}{dt} = q''_{net} + \dot{m}''\Delta h_p. \tag{28}$$

Substituting Eq. (27) into Eq. (28) and integrating yields:

$$-\frac{\rho_B c_{pB}}{3k_C L}\frac{d}{dt}[q''_{net}(L - x_c)^3] + \frac{\rho_C c_{pC}}{6k_C L}\frac{d}{dt}[q''_{net}(3Lx_c^2 - 2x_c^3)] = q''_{net} + \dot{m}''\Delta h_p. \tag{29}$$

Rearranging the above equation and performing approximate time integration between $t_{p,ini}$ and t, we get:

$$\rho_C c_{pC} q''_{net}(3Lx_c^2 - 2x_c^3) - 2\rho_B c_{pB} q''_{net}(L - x_c)^3 + 2\rho_B c_{pB} q''_{p,ini} L^3 = 3k_C L(q''_{net} + \dot{m}''\Delta h_p + q''_{p,ini})(t - t_{p,ini}). \tag{30}$$

Eq. (30) can further be reshaped to read:

$$t = t_{p,ini} + \frac{\rho_C c_{pC} q''_{net}(3Lx_c^2 - 2x_c^3) - 2\rho_B c_{pB} q''_{net}(L - x_c)^3 + 2\rho_B c_{pB} q''_{p,ini} L^3}{3k_C L(q''_{net} + \dot{m}''\Delta h_p + q''_{p,ini})}. \tag{31}$$

It is possible to estimate the pyrolysis time using Eq. (31). The pyrolysis process ceases when the char penetration depth x_c equals L. At this moment, the mass loss rate is zero. Thus, inserting $x_c = L$ and $\dot{m}'' = 0$ into Eq. (31) leads to a simple relationship for estimating the pyrolysis time.

$$t_p = t_{p,ini} + \frac{L^2(\rho_C c_{pC} q''_p + 2\rho_B c_{pB} q''_{p,ini})}{3k_C(q''_p + q''_{p,ini})}, \tag{32}$$

where q''_p denotes the net surface heat flux at the time of complete conversion of the particle. To determine its value, one needs to solve Eq. (2) together with an equation for the surface temperature at time t_p to be obtained from Eq. (27) with $x = 0$ and $x_c = L$,

$$T_{sp} = T_p + \frac{q''_p L}{2k_C}. \tag{33}$$

In Eq. (32), $t_{p,ini}$ can be well-estimated using Eq. (15), and q''_p is calculated from Eqs. (2) and (33). The rest of the parameters appearing in Eq. (32) are in fact treated as the problem input. In the forthcoming section, we will discuss that the usefulness of Eq. (32) is not limited to only approximating the pyrolysis time. In fact, it may further allow one to predict the mass loss history of a particle.

Under special circumstances and depending on the operational conditions, the net surface heat flux may approach zero. In this case, Eq. (32) simply reduces to:

$$t_p = t_{p,ini} + \frac{2L^2\rho_B c_{pB}}{3k_C}. \tag{34}$$

Eqs. (32) and (34) reveal that the pyrolysis time is proportional to the biomass density and to the square of the particle size. We arrived at a similar conclusion in a previous study [2] in which it was shown by means of a comprehensive pyrolysis model [1] that the total conversion time of a pyrolyzing biomass particle varies linearly with the initial particle density and it changes in a quadratic functional form with the particle size. From a physical point of view, the higher the heat capacitance of the biomass, i.e. $\rho_B c_{pB}$, the longer the duration of the char layer movement in order to completely penetrate into the particle. Indeed, a biomass particle with a higher heat capacitance requires longer time in order to absorb a certain amount of heat. On the other hand, it can be seen in Eqs. (32) and (34) that the pyrolysis time is proportional to the inverse of char thermal conductivity. This is because at higher values of k_C, the heat received at the surface of the particle rapidly transfers through the char layer so the heat transfer rate into the biomass layer becomes faster.

3.4. *Post-pyrolysis heating up*

Upon completion of the pyrolysis, the particle becomes completely char so that the problem reduces to a simple conduction heat transfer problem (Fig. 2d). Therefore, the solution of the post-pyrolysis process would be identical to that of the second phase of biomass heating up as described in Section 3.2 with the difference that all thermo-physical properties should be replaced with those of char. Thus, the temperature profile and the surface temperature are obtained as follows:

$$T = T_s - \frac{q''_{net}}{k_C}x + \frac{q''_{net}}{2k_C L}x^2, \tag{35}$$

$$T_s = T_{sp} + (q''_{net} - q''_p)\frac{L}{3k_C} + \frac{\alpha_C}{2k_C L}(q''_{net} + q''_p)(t - t_p). \tag{36}$$

Eq. (36) can be rearranged as follows:

$$t - t_p = \frac{T_s - T_{sp} - (q''_{net} - q''_p)(L/3k_C)}{(\alpha_C/2k_C L)(q''_{net} + q''_p)}. \tag{37}$$

At the final moment of the post-pyrolysis heating stage, the surface temperature is equal to reactor temperature T_r, so there would exist thermal equilibrium between the particle and the surrounding, implying a zero net heat flux at the surface of the particle. Thus, Eq. (37) would reduce to:

$$t_{ph} = t_f - t_p = \frac{T_r - T_{sp} + (q''_p L/3k_C L)}{(\alpha_C q''_p/2k_C L)}, \tag{38}$$

where t_{ph} denotes the duration of the post-pyrolysis heating up stage.

Eliminating q''_p between Eqs. (33) and (38), we find:

$$t_{ph} = \frac{L^2}{\alpha_C}\left(\frac{T_r - T_{sp}}{T_{sp} - T_p} + \frac{2}{3}\right). \tag{39}$$

It can be inferred from Eq. (39) that the minimum duration of the post-pyrolysis stage would occur if $T_{sp} = T_r$. Hence,

$$t_{ph} \geq \frac{2L^2}{3\alpha_C} \tag{40}$$

It has been observed from detailed numerical models [2,4,15,16] that the trend of mass loss history of small biomass particles at high temperatures is almost linear. We will later show that the mass loss history predicted by the double-temperature profile model also approximately obeys a linear function. Since the final particle density is treated as a known parameter in the present study (as well as in most simple pyrolysis models; e.g. a model based on the global one-step kinetics), one may locate the starting and ending points of mass loss curve in a mass loss-time plot, as illustrated in Fig. 5. The initiation of the pyrolysis would correspond to a mass loss of zero and the time $t_{p,ini}$ to be estimated using Eq. (15). Furthermore, the end point of the mass loss history graph would correspond to $1 - \rho_C/\rho_B$, and the time t_p to be obtained from Eq. (32). The mass loss versus time would simply be a line connecting the above two points on a mass loss-time plot. The last stage of the process; i.e. post-pyrolysis heating, is the location $(1 - \rho_C/\rho_B, t_p + t_{ph})$ as depicted in Fig. 5. It will be shown in the next section that mass loss graphs obtained from this method are well comparable with those resulted from a comprehensive pyrolysis model. Given the simplicity of this method for predicting the mass loss history, it does not provide a prediction of the mass loss *rate* history. Rather, it gives an average rate of mass loss flux throughout the process defined as $(m''_0 - m''_f)/(t_p - t_{p,ini})$ where $m'' = \rho L$ represents the particle mass per surface area. Hence,

$$\dot{m}''_{ave} = \frac{3k_C(\rho_B - \rho_c)(q''_p + q''_{p,ini})}{L(\rho_C c_{pC} q''_p + 2\rho_B c_{pB} q''_{p,ini})}. \tag{41}$$

It is also possible to provide an approximate time evolution of the surface temperature with a similar procedure. As outlined above, the duration of various stages depicted in Fig. 2; i.e. t_L, $t_{p,ini}$, t_p, t_f can be determined using the appropriate relationships presented in previous sections. On the other hand, the corresponding surface temperatures; i.e. T_L, T_p, T_{sp}, T_f, are either already known (T_p and T_f) or can be determined. Thus, a line connecting $(T_0, 0)$, (T_{sL}, t_L), $(T_p, t_{p,ini})$, (T_{sp}, t_p), (T_f, t_f) would provide an approximation of the surface temperature history (Fig. 6).

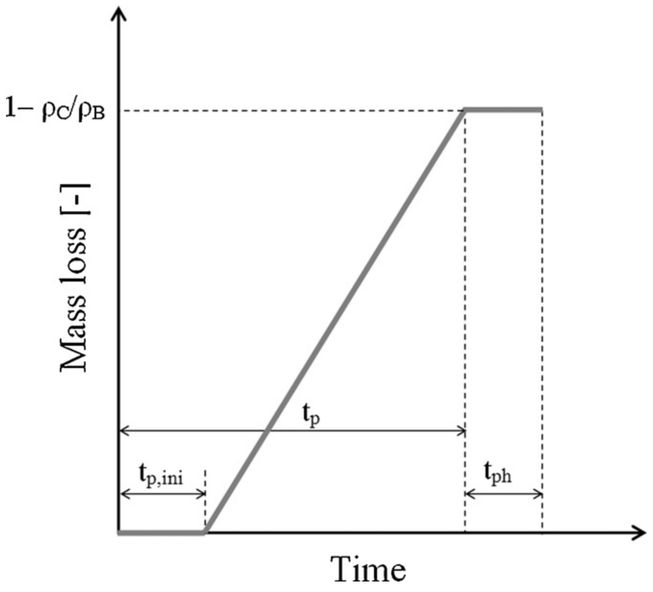

Fig. 5. Schematic diagram for predicting the mass loss history based on the single-temperature profile approach.

3.5. Numerical solution

To provide a convenient means for designers, the calculation procedure of a thermally thin particle using the proposed model with pyrolysis stage formulated based on the double-temperature profile approach is illustrated in Fig. 7. The advantage of this model compared to the one based on the single-temperature profile treatment is that it allows calculating the history of mass loss rate and

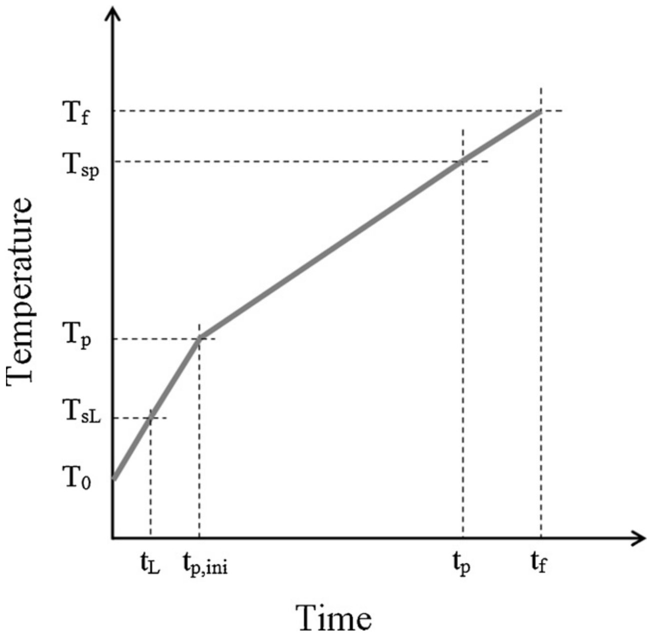

Fig. 6. Schematic diagram for predicting the surface temperature history based on the single-temperature profile approach.

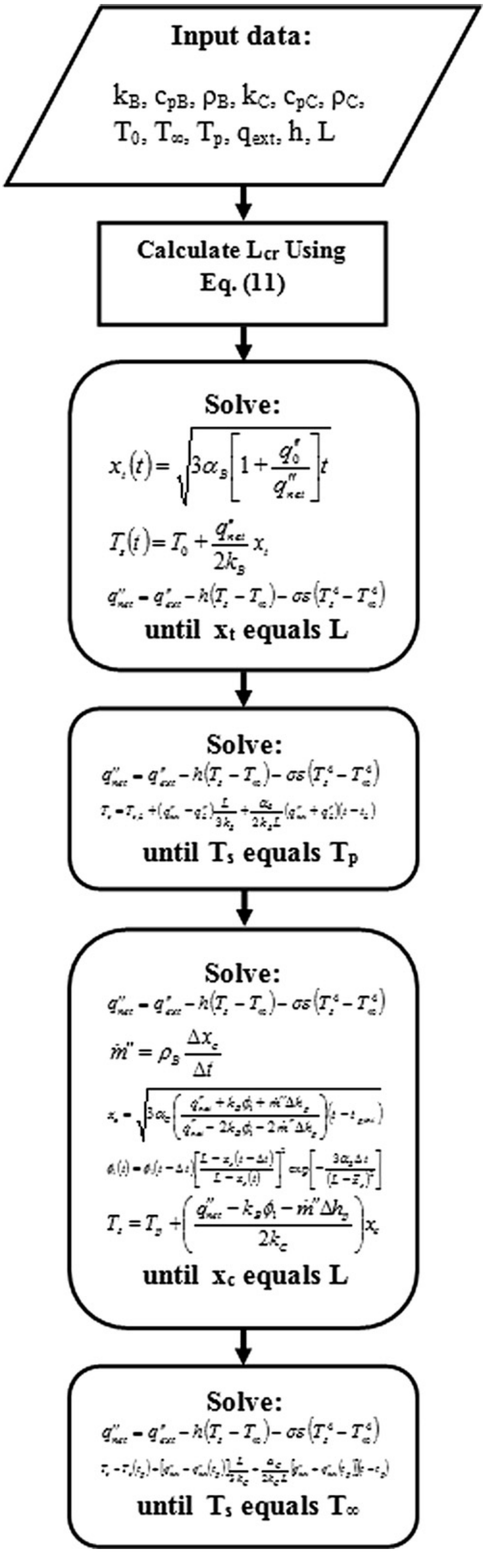
Input data:
k_B, c_{pB}, ρ_B, k_C, c_{pC}, ρ_C,
T_0, T_∞, T_p, q_{ext}, h, L
Calculate L_{cr} Using Eq. (11)
Solve:
$x_t(t)=\sqrt{3\alpha_B\left[1+\frac{q''_0}{q''_{net}}\right]t}$
$T_s(t)=T_0+\frac{q''_{net}}{2k_B}x_t$
$q''_{net}=q''_{ext}-h(T_s-T_\infty)-\sigma\varepsilon(T_s^4-T_\infty^4)$
until x_t equals L
Solve:
$q''_{net}=q''_{ext}-h(T_s-T_\infty)-\sigma\varepsilon(T_s^4-T_\infty^4)$
until T_s equals T_p
Solve:
$q''_{net}=q''_{ext}-h(T_s-T_\infty)-\sigma\varepsilon(T_s^4-T_\infty^4)$
$\dot{m}''=\rho_B\frac{\Delta x_c}{\Delta t}$
$T_s=T_p+\left(\frac{q''_{net}-k_B\phi_1-\dot{m}''\Delta h_p}{2k_C}\right)x_c$
until x_c equals L
Solve:
$q''_{net}=q''_{ext}-h(T_s-T_\infty)-\sigma\varepsilon(T_s^4-T_\infty^4)$
until T_s equals T_∞

Fig. 7. Calculation flowchart for predicting the pyrolysis process based on the double-temperature profile approach.

other key parameters by solving the appropriate equations of each stage at incremental time steps. In the initial heating up process, one needs to simultaneously solve Eqs. (2), (7) and (8). The calculations continue until x_t equals L at the characteristic time t_L. Upon satisfaction of $x_t = L$, Eqs. (2) and (14) are solved to compute the net heat flux and the temperature at the surface of the particle during the pre-pyrolysis heating up stage. When the surface temperature attains an assigned pyrolysis temperature at the time $t_{p,ini}$, the solution algorithm switches so that Eqs. (2), (21), (23), (25) and (26) are solved numerically through a trial-and-error method until x_c equals L. Finally, Eqs. (2) and (36) are solved until establishment of thermal equilibrium between particle and surrounding.

4. Results and discussion

The accuracy of the presented models based on an approximate time and space integral method has been examined by comparing the predictions of the model in terms of ignition/pyrolysis time; i.e. $t_{p,ini}$, mass loss history and the pyrolysis time against the experiments of different wood particles reported in the literature as well as the computations of a comprehensive model of pyrolyzing single wood particle published by the authors earlier [1,2], which was further used in a particle combustion model [29]. The thermo-physical properties employed in the simulations are those reported in the relevant sources taken for validation of the model, or given in the literature. Unlike in many past studies in which an endothermic heat of pyrolysis has been employed, in this study the correlation proposed by Milosavljevic et al. [30] is used for calculating the enthalpy of pyrolysis. It is proven to be a sufficient relationship, which allows producing accurate predictions when used in a pyrolysis model [2].

The first set of validation is related to prediction-experiment comparison of ignition time as given in Table 2. The data are obtained from Lu et al. [4] and Brescianini et al. [31]. In the experiments of Lu et al. [4], sawdust particles with equivalent thickness of 320 μm were heated up in an entrained-flow reactor maintained at 1625 K. Brescianini et al. [31] studied the ignition characteristics of plywood exposed to an incident heat flux in the range of 25–50 kW/m^2. It can be seen that the predicted values of ignition time compare well with the measured values.

The measured mass loss history of the sawdust particles was also reported by Lu et al. [4], so these data are further used for validation of the simplified pyrolysis models presented in this study. The comparison of the predicted mass loss histories using double- and single-temperature profile pyrolysis models with the measured values and the prediction of the comprehensive pyrolysis model of Lu et al. [4] is shown in Fig. 8. The results of both treatments compare very well with the model prediction of Lu et al. The trend of mass loss history and the conversion time reasonably agree with the experiments. All models exhibit a rather steeper mass loss history compared to the experimental data, which is likely due to the imperfect size and irregularity in particle shape, as pointed out by Lu et al. [4].

In a previous study by Haseli et al. [2], the effects of particle size and external radiant heat flux on conversion time and final char yield of beech and spruce particles were studied by means of a comprehensive pyrolysis model. The detailed description of this model can be found in Refs. [1,2]. The comprehensive model, validated against a wide range of experiments, allows one to observe time and space evolution of many parameters such as temperature, solid density, gas phase density, porosity, velocity of gaseous flow within the pores, etc. The conversion times of beech and spruce wood slab particles predicted by the simplified models of this study and the comprehensive model are illustrated in Figs. 9 and 10, respectively.

Figs. 9a and 10a illustrate comparisons between these models for an incident heat flux of 100 kW/m^2 and varying particle size. Simulations were carried out for the situation that both front surface and back face of particle are exposed to the above heat flux, so that the calculations were performed for half of the particle assuming a symmetry condition at the particle center. The comparisons shown in Figs. 9a and 10a reveal the capability of

Table 2
Comparison of the predicted and measured ignition time.

	Wood type	Plywood	Plywood	Plywood	Sawdust
	Size [mm]	11.5	11.5	11.5	0.16
	Density [kg/m^3]	550	550	550	650
	T_p [K]	673	673	673	573
External heating	q''_{ext} [kW/m^2]	25	35	50	–
	T_r [K]	–	–	–	1625
t_{ig} [s]	Measured	113 ± 20	45 ± 4	22 ± 6	0.075
	Calculated	133.8	48.2	20.1	0.089
	Source of data	Brescianini et al. (2003)			Lu et al. (2010)

the simplified models for predicting the conversion time of small particles. In order to indicate the effect of the external heating condition, another comparison is made in terms of the conversion time for a 1 mm particle at varying external heat flux, as depicted in Figs. 9b and 10b. As can be seen, the simplified models predictions in both cases are comparable with the computations of the comprehensive model. These results indicate that the new models introduced in this paper can be effectively used for practical design purposes.

The validation shown in Figs. 9 and 10 reveals that the time of pyrolysis, an important parameter for reactor engineering, can be well predicted by the simplified models. So, it can be concluded that the formulation presented for the thermally thin particle provides a useful modeling tool which can be as accurate as the comprehensive model. The main advantage of the simplified models compared to the comprehensive model is that it can be easily implemented into a reactor model and solved much quicker. In industrial reactors such as fluidized beds and entrained-flow reactors, a designer needs to deal with thermochemical conversion of a large number of small particles. The most important parameters to be calculated from a single particle model are the history of temperature and net heat flux at the surface, and mass loss. The results of this study show that the time and space integral model can be treated as a useful tool for engineering applications.

In real furnaces, the shape of particles could be far from a slab and they may be cylindrical and/or spherical-like. Therefore, it is worth extending the analysis of the time and space integral method to the shapes other than a slab. The derivation of the key relationships would be very much similar to that presented for a slab particle. However, one should realize that unlike slab particles in that the heat transfer area is identical along the particle, in a cylindrical and/or spherical particle the heat transfer area consistently decreases from its maximum values being at the surface to the center of particle where the surface area is zero. This has to be accounted for when performing space integration

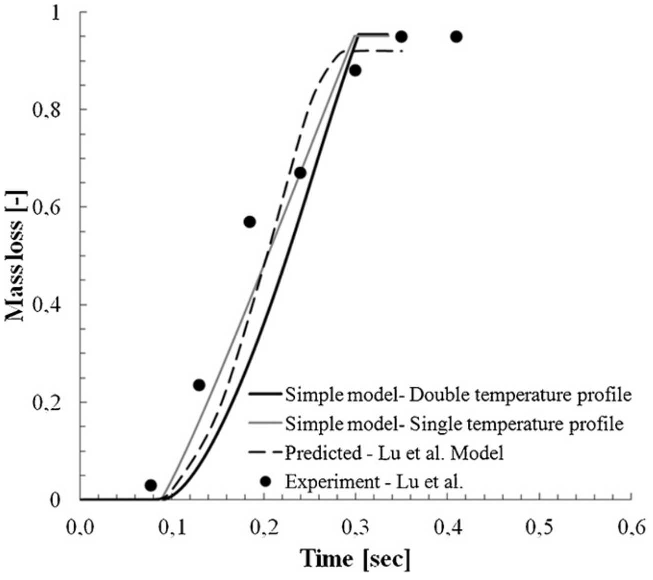

Fig. 8. Comparison of the prediction of the simple models with the experiment and the prediction of Lu et al. model [4] (L = 160 μm and T_r = 1625 K).

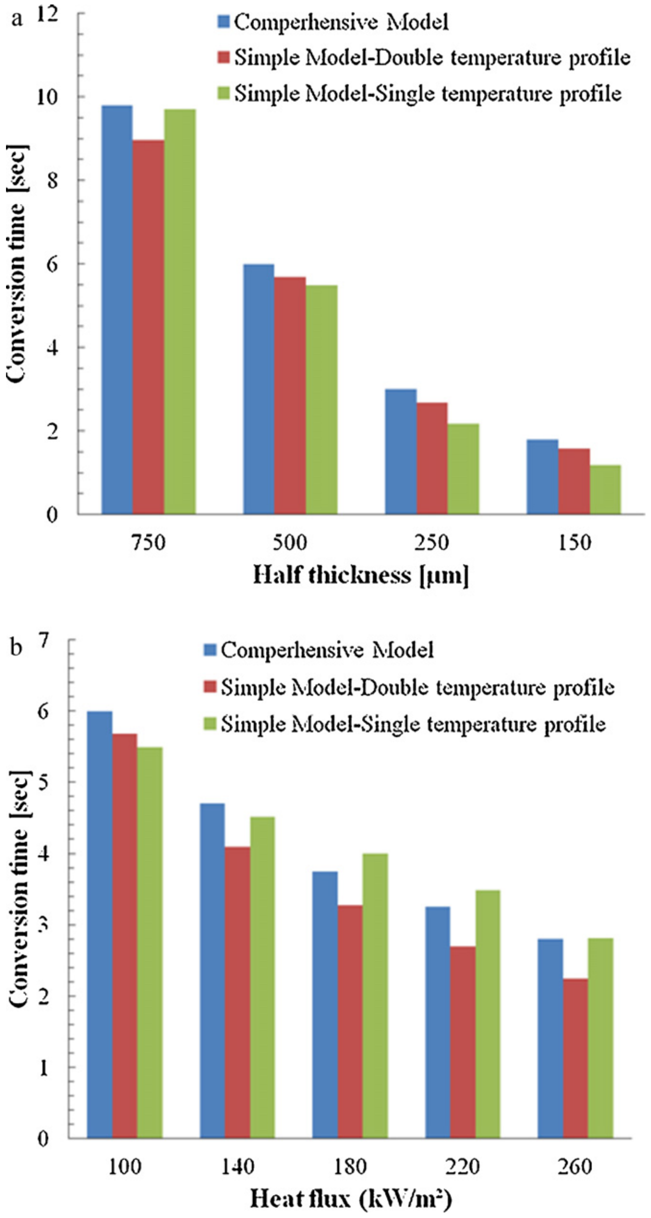

Fig. 9. Conversion time of beech wood particle predicted by a comprehensive model and the simplified model: (a) conversion time versus particle half thickness q''_{ext} = 100 kW/m^2; (b) conversion time of a 1 mm particle versus heat flux.

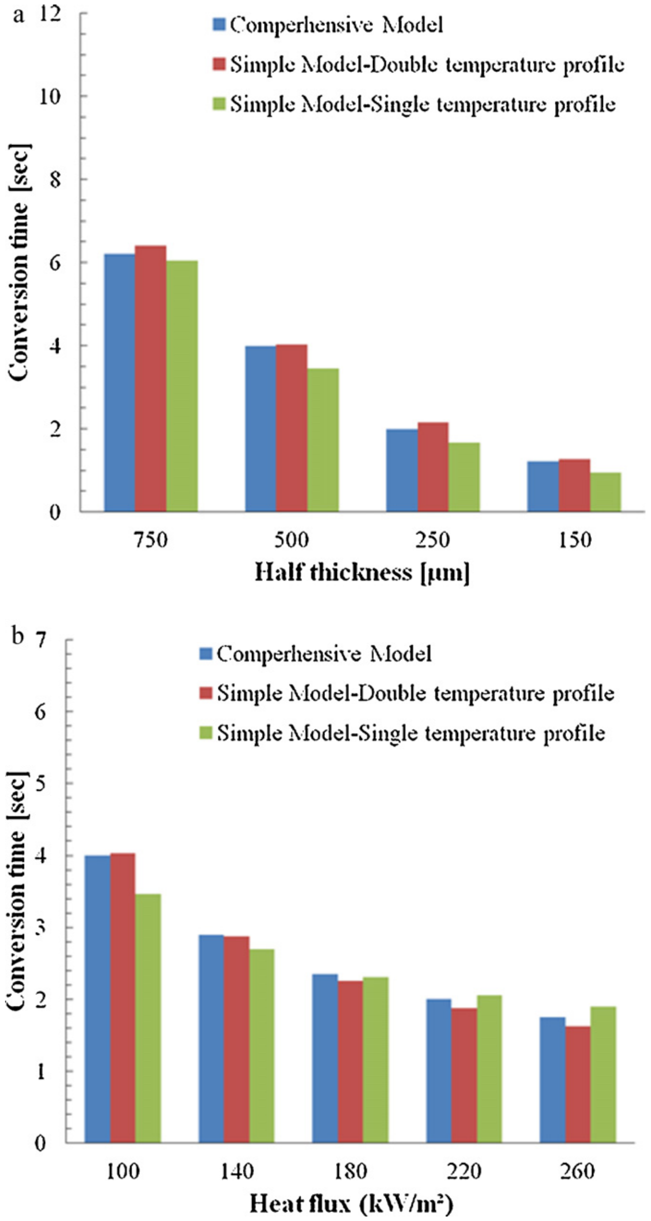

Fig. 10. Conversion time of spruce wood particle predicted by a comprehensive model and the simplified model: (a) conversion time versus particle half thickness $q''_{\mathrm{ext}} = 100\ \mathrm{kW/m^2}$; (b) conversion time of a 1 mm particle versus heat flux.

of the heat transfer equations in all stages of the process described previously.

Below, we present the expressions for computation of time of pyrolysis initiation, pyrolysis time and post-pyrolysis heating up duration suitable for cylindrical/spherical particles. The objective is to provide plant engineers and designers with simple relationships to help them estimate preheating and pyrolysis time as well as mass loss history. The form of the results for cylindrical and spherical particles is the same as those of slab, but with different numerical constants. In general, the relationships for evaluating the durations of preheating, pyrolysis and post-pyrolysis heating are as follows:

$$t_{\mathrm{p,ini}} = \frac{R^2}{C_1\alpha_{\mathrm{B}}(1+(q''_0/q''_R))} + \frac{C_2 k_{\mathrm{B}} R(T_{\mathrm{p}} - T_{\mathrm{sR}}) - (C_2/C_1)(q''_{\mathrm{p}} - q''_{\mathrm{R}})R^2}{\alpha_{\mathrm{B}}(q''_{\mathrm{p}} + q''_{\mathrm{R}})}, \tag{42}$$

$$t_{\mathrm{p}} = t_{\mathrm{p,ini}} + \frac{R^2(\rho_{\mathrm{C}} c_{\mathrm{pC}} q''_{\mathrm{p}} + C_2 \rho_{\mathrm{B}} c_{\mathrm{pB}} q''_{\mathrm{p,ini}})}{C_1 k_{\mathrm{C}}(q''_{\mathrm{p}} + q''_{\mathrm{p,ini}})}, \tag{43}$$

$$t_{\mathrm{ph}} = \frac{R^2}{\alpha_{\mathrm{C}}}\left(\frac{C_2}{2}\frac{T_{\mathrm{r}} - T_{\mathrm{sp}}}{T_{\mathrm{sp}} - T_{\mathrm{p}}} + \frac{C_2}{C_1}\right), \tag{44}$$

where for a cylinder ($C_1 = 4$, $C_2 = 1$) and a sphere ($C_1 = 5$, $C_2 = 2/3$). Looking back into Eqs. (15), (32) and (39) one may realize that for a slab $C_1 = 3$ and $C_2 = 2$. Notice that the relationship for estimating the pyrolysis time; i.e. Eq. (43), is obtained based on the single-temperature profile approach.

The accuracy of this model for prediction of the mass loss of cylindrical and spherical particles is assessed using the data of Lu et al. [4], who investigated the effect of particle shape on the pyrolysis of small particles. In their study, cylindrical and spherical-like sawdust particles with equivalent diameter of 320 μm and nearly the same mass and volume were pyrolyzed at 1625 K. The aspect ratios of the cylindrical-like and spherical-like particles were 6 and 1.65, respectively. Fig. 11 compares the prediction of the simple model with the experiments and the model prediction of Lu et al. [4] for both cylindrical and near-spherical particles. As evident from Fig. 11, in both cases the simple model prediction compares well quantitatively and qualitatively with the prediction of a comprehensive model and the measured mass loss history. A further observation from this figure is that the spherical-like particle pyrolyzes slower than the cylindrical particle does, which is due to the lower surface area-to-volume of the near-spherical particle than the cylindrical sawdust species. Lu et al. [4] developed a 3-D particle shape reconstruction algorithm to measure and calculate particle surface area and volume. The measured external surface area for slab-like, cylindrical and near-spherical particles was 0.491 mm^2, 0.479 mm^2 and 0.344 mm^2, respectively.

We place an emphasis on the key parameter which needs to be carefully assigned a constant value; i.e. the pyrolysis temperature T_{p}. Despite that this parameter may not exactly represent the real temperature at which the decomposition takes place, it greatly facilitates simplification of a pyrolysis model compared to the case in which it is calculated from a finite-rate kinetics; e.g. Ref. [25,26]. Given that a wide range of values has been reported in the literature, T_{p} should be treated as an adjustable parameter leading to results comparable with experiments or prediction of a detailed model based on finite rate kinetics [28].

Past studies by Spearpoint and Quintiere [23,32] indicated that T_{p} obtained from experimental tests is material and orientation dependent. They discovered that when the external heat flux was along the grain, the ignition temperatures were much greater than those obtained for the case that the incident heat flux was radiated across the grain. For instance, they determined average ignition temperatures of 375 °C and 204 °C for Redwood for the external heat flux radiating along and across the grain, respectively. Another study by Moghtaderi et al. [33] revealed that the ignition temperature depends on the external heat flux and moisture content. They measured ignition temperatures for Radiata pine wood for incident heat flux of 20–60 kW/m^2 and moisture content of 0–30%, and found a range of 298 °C–400 °C. Moreover, Yang et al. [34] reported a range of 190 °C–310 °C for the ignition temperature of wood. As a result, a designer needs to carefully select a proper value for the pyrolysis temperature otherwise it may lead to insufficient accuracy of the simplified models predictions. If experimental data is available, it is suggested to assign a measured value for T_{p}, otherwise the correlation proposed by Park et al. [35] may be employed as a useful tool which allows one to estimate T_{p} as a function of process parameters such external heat flux and particle size.

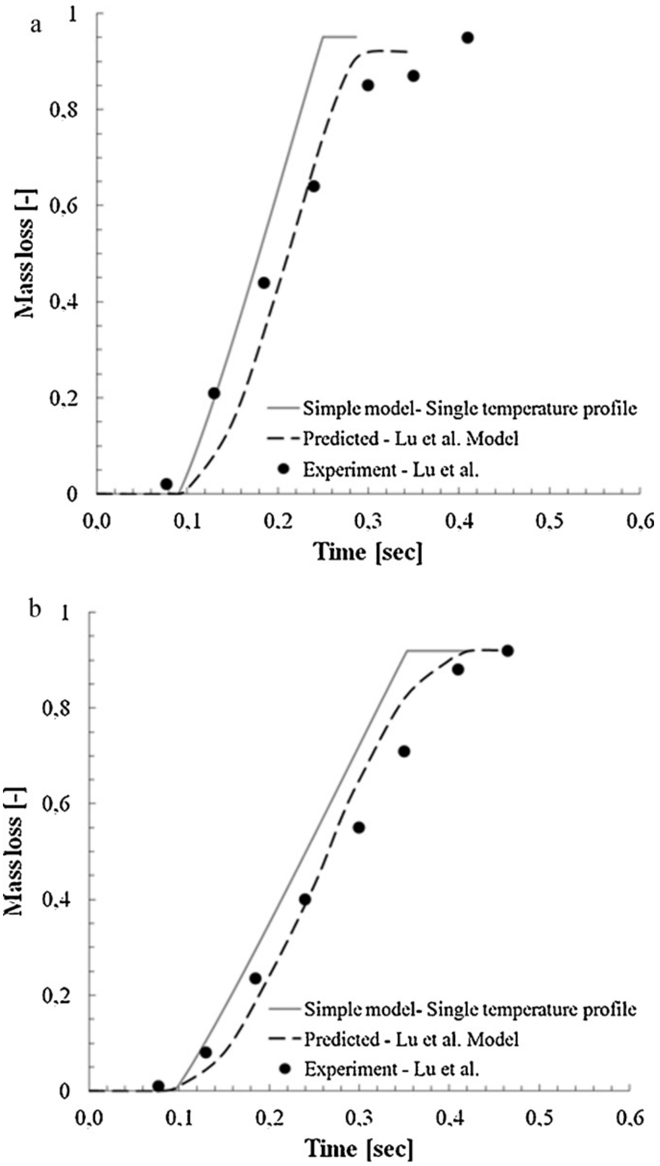

Fig. 11. Comparison of the prediction of the simple model with the experiment and the prediction of Lu et al. model [4]: (a) cylindrical-like particle; (b) spherical-like particle (d_{eq} = 320 μm, T_r = 1625 K).

5. Conclusion

A simple pyrolysis model for a thermally thin biomass particle is developed based on a time and space integral method, which has not been previously presented in the literature. The model is based on the main assumptions of constant thermo-physical properties, decomposition of biomass according to a shrinking core model at a thin reaction layer at a prescribed pyrolysis temperature, and approximating the spatial temperature profile with a polynomial function. The formulation of various stages of the conversion process has been presented using the time and space integral method resulting in transformation of partial differential form of heat transfer equation into an algebraic equation.

Two different treatments were presented. The first formulation allows one to compute the history of key process parameters such as net heat flux at the surface, mass loss rate, char penetration depth and particle weight loss according to the calculation algorithm presented in Fig. 7. This model may, for example, be used in combustor and gasifier design codes where a large number of biomass particles undergo a thermal decomposition, since computationally it is cheaper and easier to implement in a CFD code than comprehensive models. On the other hand, the second treatment provides rather simple relationships for estimating the duration of various stages of the process including preheating, pyrolysis and post-pyrolysis heating. This method can be the interest of plant engineers since it provides a simple but useful tool to sufficiently predict the mass loss history of a pyrolyzing particle (see Fig. 5). Also, time evolution of the surface temperature can be approximated using the method illustrated in Fig. 6.

Typical experimental data related to the mass loss history of sawdust particles reported in the literature are used to examine the accuracy of the presented models. The predictions are found to be in a good agreement both quantitatively and qualitatively with the experimental data as well as the prediction of comprehensive numerical models. Additional validation is carried out using the prediction of the comprehensive pyrolysis model previously published by the authors [1,2] in terms of the conversion time of beech and spruce wood particles. The predictions of both treatments based on the time and space integral model agree well with the results of the comprehensive model. The key conclusion is that if the thermo-physical properties are assigned proper values, the pyrolysis models based on double- and single-temperature profile can be effectively used in practical applications.

Acknowledgment

The financial support provided by the Dutch Technology Foundation STW through project BiOxyFuel No. 10416 is gratefully acknowledged.

References

[1] Y. Haseli, J.A. van Oijen, L.P.H. de Goey, Modeling biomass particle pyrolysis with temperature-dependent heat of reactions, Journal of Analytical and Applied Pyrolysis 90 (2011) 140–154.
[2] Y. Haseli, J.A. van Oijen, L.P.H. de Goey, Numerical study of the conversion time of single pyrolyzing biomass particles at high heating conditions, Chemical Engineering Journal 169 (2011) 299–312.
[3] Y. Haseli, J.A. van Oijen, L.P.H. de Goey, Pyrolysis time correlation for a single biomass particle exposed to high temperatures, in: Proceedings of 3rd IEEE Asia–Pacific Power and Energy Engineering Conference, 25–28 March 2011, Wuhan, China, 2011.
[4] H. Lu, E. Ip, J. Scott, P. Foster, M. Vickers, L.L. Baxter, Effects of particle shape and size on devolatilization of biomass particle, Fuel 89 (2010) 1156–1168.
[5] W.C. Park, A. Atreya, H.R. Baum, Experimental and theoretical investigation of heat and mass transfer processes during wood pyrolysis, Combustion and Flame 157 (2010) 481–494.
[6] K. Papadikis, S. Gu, A.V. Bridgwater, CFD modelling of the fast pyrolysis of biomass in fluidised bed reactors: modelling the impact of biomass shrinkage, Chemical Engineering Journal 149 (2009) 417–427.
[7] K. Papadikis, S. Gu, A.V. Bridgwater, H. Gerhauser, Application of CFD to model fast pyrolysis of biomass, Fuel Processing Technology 90 (2009) 504–512.
[8] O. Authier, M. Ferrer, G. Mauviel, A.E. Khalfi, J. Lede, Wood fast pyrolysis: comparison of Lagrangian and Eulerian modeling approaches with experimental measurements, Industrial and Engineering Chemistry Research 48 (2009) 4796–4809.
[9] A.K. Sadhukhan, P. Gupta, R.K. Saha, Modeling of pyrolysis of large wood particles, Bioresource Technology 100 (2009) 3134–3139.
[10] A.K. Sadhukhan, P. Gupta, R.K. Saha, Modeling and experimental studies on pyrolysis of biomass particles, Journal of Analytical and Applied Pyrolysis 81 (2008) 183–192.
[11] C. Di Blasi, Modeling chemical and physical processes of wood and biomass pyroysis, Progress in Energy and Combustion 34 (2008) 47–90.
[12] M. Sreekanth, A.K. Kolar, B. Leckner, Transient thermal behaviour of a cylindrical wood particle during devolatilization in a bubbling fluidized bed, Fuel Processing Technology 89 (2008) 838–850.
[13] C. Ghabi, H. Benticha, M. Sassi, Two-dimensional computational modeling and simulation of wood particles pyrolysis in a fixed bed reactor, Combustion Science and Technology 180 (2008) 833–853.
[14] H. Lu, W. Robert, G. Peirce, B. Ripa, L.L. Baxter, Comprehensive study of biomass particle combustion, Energy Fuels 22 (2008) 2826–2839.
[15] A. Bharadwaj, L.L. Baxter, A.L. Robinson, Effects of intraparticle heat and mass transfer on biomass devolatilization: experimental results and model predictions, Energy Fuels 18 (2004) 1021–1031.

[16] J. Saastamoinen, M. Aho, A. Moilanen, L.H. Sørensen, S. Clausen, M. Berg, Burnout of pulverized biomass particles in large scale boiler—single particle model approach, Biomass Bioenergy 34 (2010) 728–736.
[17] T.R. Goodman, Application of integral method to transient nonlinear heat transfer, in: T.F. Irvine, J.P. Hartnelt (Eds.), Advances in Heat Transfer, Academic Press, New York, 1964, pp. 51–122.
[18] A.M. Kanury, Rate of burning of wood (a simple thermal model), Combustion Science and Technology 5 (1972) 135–146.
[19] A.M. Kanury, D.J. Holve, Transient conduction with pyrolysis (Approximate solutions for charring wood slabs), Journal of Heat Transfer 104 (1982) 338–343.
[20] Y. Chen, M.A. Delichatios, V. Motevalli, Material pyrolysis properties, part I: an integral model for one-dimensional transient pyrolysis of charring and non-charring materials, Combustion Science and Technology 88 (1993) 309–328.
[21] J. Quintiere, N. Iqbal, An approximate integral model for the burning rate of a thermoplastic-like material, Fire and Materials 18 (1994) 89–98.
[22] W.G. Weng, Y. Hasemi, W.C. Fan, Predicting the pyrolysis of wood considering char oxidation under different ambient oxygen concentrations, Combustion and Flame 145 (2006) 723–729.
[23] M.J. Spearpoint, J.G. Quintiere, Predicting the burning of wood using an integral model, Combustion and Flame 123 (2000) 308–324.
[24] B. Moghtaderi, The state-of-the-art in pyrolysis modelling of lignocellulosic solid fuels, Fire and Materials 30 (2006) 1–34.
[25] A. Galgano, C. Di Blasi, Modeling wood degradation by the unreacted core shrinking approximation, Industrial and Engineering Chemistry Research 42 (2003) 2101–2111.
[26] A. Galgano, C. Di Blasi, Modeling the propagation of drying and decomposition fronts in wood, Combustion and Flame 139 (2004) 16–27.
[27] F. Jia, E.R. Galea, M.K. Patel, Numerical simulation of the mass loss process in pyrolizing char materials, Fire and Materials 23 (1999) 71–78.
[28] A. Galgano, C. Di Blasi, Infinite versus finite rate kinetics in simplified models of wood pyrolysis, Combustion Science and Technology 177 (2005) 279–303.
[29] Y. Haseli, J.A. van Oijen, L.P.H. de Goey, A detailed one-dimensional model of combustion of a woody biomass particle, Bioresource Technology 102 (2011) 9772–9782.
[30] I. Milosavljevic, V. Oja, E.M. Suuberg, Thermal effects in cellulose pyrolysis: relationship to char formation processes, Industrial and Engineering Chemistry Research 35 (1996) 653–662.
[31] C.P. Brescianini, M.A. Delichatsios, A.K. Webb, Mathematical modeling of time to ignition in the early fire hazard test, Combustion Science and Technology 175 (2003) 319–331.
[32] M.J. Spearpoint, J.G. Quintiere, Predicting the piloted ignition of wood in the cone calorimeter using an integral model—effect of species, grain orientation and heat flux, Fire Safety Journal 36 (2001) 391–415.
[33] B. Moghtaderi, V. Novozhilov, D. Fletcher, J.H. Kent, A new correlation for bench-scale piloted ignition data of wood, Fire Safety Journal 29 (1997) 41–59.
[34] L. Yang, X. Chen, X. Zhou, W. Fan, The pyrolysis and ignition of charring materials under an external heat flux, Combustion and Flame 133 (2003) 407–413.
[35] W.C. Park, A. Atreya, H.R. Baum, Determination of pyrolysis temperature for charring materials, Proceedings of the Combustion Institute 32 (2009) 2471–2479.